Comparative CO_2 flux measurements by eddy covariance technique using open- and closed-path gas analysers over the equatorial Pacific Ocean

By FUMIYOSHI KONDO[1,2]* and OSAMU TSUKAMOTO[1], [1]*Graduate School of Natural Science and Technology, Okayama University, Okayama 700-8530, Japan; [2]Atmosphere and Ocean Research Institute, The University of Tokyo, Tokyo 277-8564, Japan*

Direct comparison of air–sea CO_2 fluxes by open-path eddy covariance (OPEC) and closed-path eddy covariance (CPEC) techniques was carried out over the equatorial Pacific Ocean. Previous studies over oceans have shown that the CO_2 flux by OPEC was larger than the bulk CO_2 flux using the gas transfer velocity estimated by the mass balance technique, while the CO_2 flux by CPEC agreed with the bulk CO_2 flux. We investigated a traditional conflict between the CO_2 flux by the eddy covariance technique and the bulk CO_2 flux, and whether the CO_2 fluctuation attenuated using the closed-path analyser can be measured with sufficient time responses to resolve small CO_2 flux over oceans. Our results showed that the closed-path analyser using a short sampling tube and a high volume air pump can be used to measure the small CO_2 fluctuation over the ocean. Further, the underestimated CO_2 flux by CPEC due to the attenuated fluctuation can be corrected by the bandpass covariance method; its contribution was almost identical to that of H_2O flux. The CO_2 flux by CPEC agreed with the total CO_2 flux by OPEC with density correction; however, both of them are one order of magnitude larger than the bulk CO_2 flux.

Keywords: CO_2 flux, eddy covariance technique, open-path gas analyser, closed-path gas analyser, WPL correction

1. Introduction

Eddy covariance technique is the most direct turbulent flux measurement. This technique makes it possible to measure the flux on the same time and spatial scales as the variability of various processes that influence the trace gas flux between the air–sea interface. However, in this technique, fluxes of only three trace gases, H_2O, CO_2 and CH_4, can be directly measured using an open-path gas analyser (OPGA); the fluxes of other trace gases (SO_2, NO, NO_x, O_3) and a carbon isotope ($^{13}CO_2$) have to be indirectly measured using a closed-path gas analyser (CPGA) in which the sample air must be first drawn through a sampling tube into a sample cell.

Since the first measurement reported by Jones and Smith (1977), the turbulent CO_2 flux directly evaluated by the open-path eddy covariance (OPEC) technique over the coastal sea and open ocean was shown to be larger than the air–sea bulk CO_2 flux estimated using the gas transfer

velocity, which was evaluated by mass balance techniques using natural and bomb-produced ^{14}C, $^{222}Rn/^{226}Ra$ and $SF_6/^3He$ as tracers (Smith and Jones, 1985; Jacobs et al., 1999; Kondo and Tsukamoto, 2007). McGillis et al. (2001, 2004) reported that, in contrast, the turbulent CO_2 flux evaluated by the closed-path eddy covariance (CPEC) technique has shown almost the same value as the bulk CO_2 flux estimated using the gas transfer velocity, which was simultaneously evaluated by a mass balance technique using $SF_6/^3He$ dual tracers. Miller et al. (2010) also evaluated the turbulent CO_2 flux by the CPEC, which was converted from an original OPGA and reached the same conclusion as reported in the study by McGillis et al. (2001).

Comparative measurements of CO_2 fluxes by the OPEC and CPEC over the land were performed in the 1990s (Leuning and Moncrieff, 1990), and the results were consistent (Suyker and Verma, 1993; Lee et al., 1994; Yasuda and Watanabe, 2001; Ibrom et al., 2007b). However, over the ocean where the CO_2 density fluctuation is one order of magnitude smaller than that over the terrestrial ecosystem, comparative measurements of CO_2 fluxes using both analysers have rarely been reported.

*Corresponding author.
email: fkondo@aori.u-tokyo.ac.jp

1

The OPGA has an advantage of directly measuring the CO_2 density fluctuation in atmospheric turbulence. Considering the present sensitivity of gas analysers used over the ocean where high accuracy measurement is required, it has the other advantage of measuring the larger CO_2 density fluctuation than the fluctuation caused by air–sea CO_2 flux because of including the apparent CO_2 density fluctuation due to the air density fluctuation resulting from the air temperature and H_2O density fluctuations. In the 1970s, when the first measurement was performed (Jones and Smith, 1977), there was a question whether the CO_2 flux evaluated by the eddy covariance technique was sufficiently accurate over the ocean where the CO_2 density fluctuation is small. Recently, Kondo and Tsukamoto (2007) has reported that precise measurements of this small CO_2 density fluctuation using the present OPGA were obtained over the equatorial Indian Ocean based on detailed spectral analysis. However, the magnitude of upward density correction due to air temperature and H_2O density fluctuations the so-called Webb or WPL (Webb, Pearman and Leuning) correction, mentioned in a later section exceeded the apparent downward CO_2 flux. In contrast, the CPGA can indirectly measure the CO_2 density fluctuation in moist sample air, which is influenced by the air density fluctuation due to only the H_2O density fluctuation because the temperature fluctuation in the sample air is fully attenuated in a sampling tube from the sampling point (Sahlée and Drennan, 2009). Moreover, the CPGA can measure the CO_2 density (or mixing ratio) fluctuation in sample air that was pre-dried using a membrane dryer; therefore, it has the advantage of evaluating the CO_2 flux without the WPL correction. However, the CO_2 density fluctuation measured by the CPGA attenuates in the sampling tube. The degree of this attenuation, which leads to underestimations of the CO_2 flux, primarily depends on two factors: the length and diameter (dead volume) of the sampling tube and the airflow state (laminar or turbulent) within the tube (Leuning and Moncrieff, 1990; Lenschow and Raupach, 1991; Leuning and King, 1992). Many researchers have used a high volume air pump to keep the turbulent airflow within the sampling tube. However, the length of sampling tube is required to be long because of the constraints faced on many ships over the open ocean. When using a long sampling tube, the CPGA may not measure the attenuated smaller CO_2 density (or mixing ratio) fluctuation with a sufficient time response to resolve the CO_2 flux when using a long sampling tube to evaluate the small CO_2 flux over the ocean. McGillis et al. (2001) and Miller et al. (2010) used a long sampling tube, but they did not convincingly report whether the attenuated smaller CO_2 density (or mixing ratio) fluctuation over the ocean could be measured by the CPGA.

This study presents a direct comparison of the small CO_2 fluxes by the OPEC and CPEC over the open ocean. A fast Fourier transform spectrum analysis technique was used to demonstrate the attenuating influence of the sampling tube on the CO_2 density fluctuation measured by the CPGA. We also discuss the possibility of the underestimated flux correction (frequency correction) for the attenuated small CO_2 density fluctuation measured by the CPGA. Finally, we present a direct comparison of the CO_2 fluxes evaluated by the eddy covariance technique using both analysers in addition to the bulk CO_2 flux estimated using the gas transfer velocity by the mass balance technique.

2. Methods

2.1. Theory of CO_2 fluxes by the OPEC and CPEC techniques

The air–sea turbulent CO_2 flux by the eddy covariance technique [F_c(EC), $mg\,m^{-2}\,s^{-1}$] is given by:

$$F_c(EC) = \overline{\rho_d w r_c} = \overline{\rho_d} \cdot \overline{w' r_c'}, \tag{1}$$

where ρ_d is the dry air mass density ($kg\,m^{-3}$), w is the vertical wind velocity ($m\,s^{-1}$) and r_c is the mass mixing ratio of CO_2 relative to the dry air ($mg\,kg^{-1}$). The prime indicates the fluctuation as a deviation from the mean value (overbar) over a sampling period.

The infrared CO_2/H_2O gas analyser measures the CO_2 and H_2O densities rather than their mixing ratios because it cannot measure the air temperature and pressure at the same time and point in atmospheric turbulence. Therefore, the turbulent CO_2 flux by the eddy covariance technique is given by:

$$F_c(EC) = \overline{\rho_d w r_c} = \overline{\rho_d w \frac{\rho_c}{\rho_d}} = \overline{w \rho_c} = \overline{w' \rho_c'} + \overline{w} \overline{\rho_c}, \tag{2}$$

where ρ_c is the CO_2 mass density ($mg\,m^{-3}$). The first and second terms on the right-hand side of eq. (2) are the raw CO_2 flux and the CO_2 flux due to the mean vertical flow, respectively. Webb et al. (1980) suggested that the flux due to the mean vertical flow cannot be neglected for trace gases such as H_2O and CO_2. To evaluate the magnitude of the influence of the mean vertical flow, Webb et al. (1980) assumed that the vertical flux of dry air should be zero:

$$\overline{w \rho_d} = \overline{w} \overline{\rho_d} + \overline{w' \rho_d'} = 0. \tag{3}$$

Using the ideal gas equation, the final expression for the total CO_2 flux by the OPEC technique [F_c(OPEC), $mg\,m^{-2}\,s^{-1}$] can be written as follows:

$$F_c(OPEC) = \overline{w' \rho_{c\_op}'} + \mu \frac{\overline{\rho_{c\_op}}}{\overline{\rho_d}} \overline{w' \rho_{v\_op}'} + (1 + \mu\sigma) \frac{\overline{\rho_{c\_op}}}{\overline{T}} \overline{w' T'}, \tag{4}$$

where ρ_{c_op} and ρ_{v_op} are the CO$_2$ and H$_2$O mass densities measured by the open-path CO$_2$/H$_2$O gas analyser (mg m^{-3}), respectively, μ is the ratio of the molecular weights of dry air to those of H$_2$O (kg g^{-1}), σ is the ratio of H$_2$O density to dry air density (g kg^{-1}) and T is the absolute air temperature (K). The first, second and third terms on the right-hand side in eq. (4) are the raw CO$_2$ flux and WPL correction terms due to H$_2$O density fluctuations (related to latent heat flux, and hereafter, *WPL for LHF*) and due to air temperature fluctuations (related to sensible heat flux, and hereafter, *WPL for SHF*), respectively.

The CO$_2$ flux by the CPEC technique [F_c(CPEC), mg m^{-2} s^{-1}] can be expressed as follows (Leuning and Moncrieff, 1990; Suyker and Verma, 1993):

$$F_c(\text{CPEC}) = \left(\frac{\overline{p} \cdot \overline{T_{cl}}}{\overline{p_{cl}} \cdot \overline{T}}\right) \cdot \left[\overline{w' \rho'_{c\_cl}} + \mu \left(\frac{\overline{\rho_{c\_cl}}}{\overline{\rho_d}}\right) \overline{w' \rho'_{v\_cl}}\right], \quad (5)$$

where p and T are the air pressure and temperature, respectively, and T_{cl}, p_{cl}, ρ_{c_cl} and ρ_{v_cl} are the temperature, pressure and CO$_2$ and H$_2$O mass densities in the sample cell of the closed-path CO$_2$/H$_2$O gas analyser, respectively. Equation (5) assumes that the temperature fluctuation in the sample air is attenuated ($T' = 0$) when the air is drawn through a sampling tube. In the present study, we have adopted a closed-path CO$_2$/H$_2$O infrared gas analyser that gives the CO$_2$ and H$_2$O mole fractions as the output; they were calculated from the measured CO$_2$ and H$_2$O densities using the pressure and temperature in the sample cell. The CO$_2$ flux by the CPEC technique is thus given by Yasuda and Watanabe (2001):

$$F_c(\text{CPEC}) = \overline{\rho_d w r_c} = \overline{\rho_d} \cdot \overline{w' r'_c} = \overline{\rho_d} \cdot \overline{w' \left(\frac{\rho_c}{\rho_d}\right)'}$$

$$= \overline{\rho_d} \cdot \overline{w' \left[\frac{X_{c\_cl} \cdot m_c}{(1 - X_{v\_cl}) \cdot m_d}\right]'}, \quad (6)$$

$$X_{c\_cl} = \frac{\rho_{c\_cl}}{\rho_{a\_cl}} \cdot \frac{m_a}{m_c}, \quad (7)$$

$$X_{v\_cl} = \frac{\rho_{v\_cl}}{\rho_{a\_cl}} \cdot \frac{m_a}{m_v}, \quad (8)$$

where ρ_{a_cl} is the moist air mass density in a sample cell (kg m^{-3}), X_{c_cl} (μmol mol^{-1}) and X_{v_cl} (mmol mol^{-1}) are the CO$_2$ and H$_2$O mole fractions in the moist air in the sample cell measured by the closed-path CO$_2$/H$_2$O gas analyser, and m_c, m_d and m_a are the molecular weights of CO$_2$ (44.01 g mol^{-1}), dry air (28.97 g mol^{-1}) and moist air, respectively.

2.2. Theory of air–sea bulk CO$_2$ flux

A two-layer film model can be used for the estimation of air–sea gas flux (Liss and Merlivat, 1986). The air–sea bulk CO$_2$ flux [F_c(Bulk), mg m^{-2} s^{-1}] can be calculated from the air–sea difference in the fugacity of CO$_2$ at the surface and gas transfer velocity as follows:

$$F_c(\text{Bulk}) = k_c \cdot S_c \cdot \Delta f\text{CO}_2, \quad (9)$$

where k_c (m s^{-1}) is the gas transfer velocity of CO$_2$ modified by the Schmidt number, S_c (mg m^{-3} μatm^{-1}) is the solubility of CO$_2$, which depends on the salinity and seawater temperature (Weiss, 1974) and ΔfCO$_2$ (μatm) is the difference between the fugacities of CO$_2$ in bulk seawater and air, respectively. The layer thickness controls the gas transfer velocity and depends significantly on the wind speed. Empirical equations describe the gas transfer velocity as a function of wind speed. Variety parameterisations have been proposed to calculate the gas transfer velocity of CO$_2$. In this study, we have adopted the gas transfer velocity proposed by Wanninkhof (1992), which was evaluated by the mass balance technique using the tracers of the natural and bomb-produced ^{14}C, ^{222}Rn/^{226}Ra and SF$_6$/^{3}He. Wanninkhof (1992) proposed the gas transfer velocity, $k_c = 0.31 U^2$, where U is the wind speed. We estimated the bulk CO$_2$ flux at each station using the mean wind speed and ΔfCO$_2$ for the period during which flux observation runs were performed.

2.3. Instrumentation

We installed turbulent flux and ship motion correction systems on top of the foremast (approximately 24 m above the mean sea surface) of the R/V MIRAI, as shown in Fig. 1. The turbulent flux system consisted of a sonic anemometer-thermometer (SAT) (KAIJO, DA-600-3TV) for measuring the fluctuations of three wind velocities and sound virtual temperature as well as the infrared open-path (LI-COR, LI-7500) and closed-path (LI-COR, LI-7000) CO$_2$/H$_2$O gas analysers for measuring the fluctuations of the CO$_2$ and H$_2$O densities and mole fractions, respectively. A diaphragm air pump (Yasunaga Air Pump, YP-30VC) was used to draw the sample air from the sampling point near the OPGA and SAT through a nylon tube (3.2 m long, 1/4 inch in diameter) to the sample cell of the CPGA. In this study, we used a short sampling tube because of focusing on the difference in theory between the CO$_2$ fluxes by the OPEC and CPEC. The flow rate to the sample cell of CPGA was maintained at 12.0 L min^{-1} with a mass flow controller (Kofloc, RK1250). The theoretical CPGA lag time for CO$_2$ and H$_2$O due to the travel time in the sampling tube, which was calculated from the inner diameter and length of the
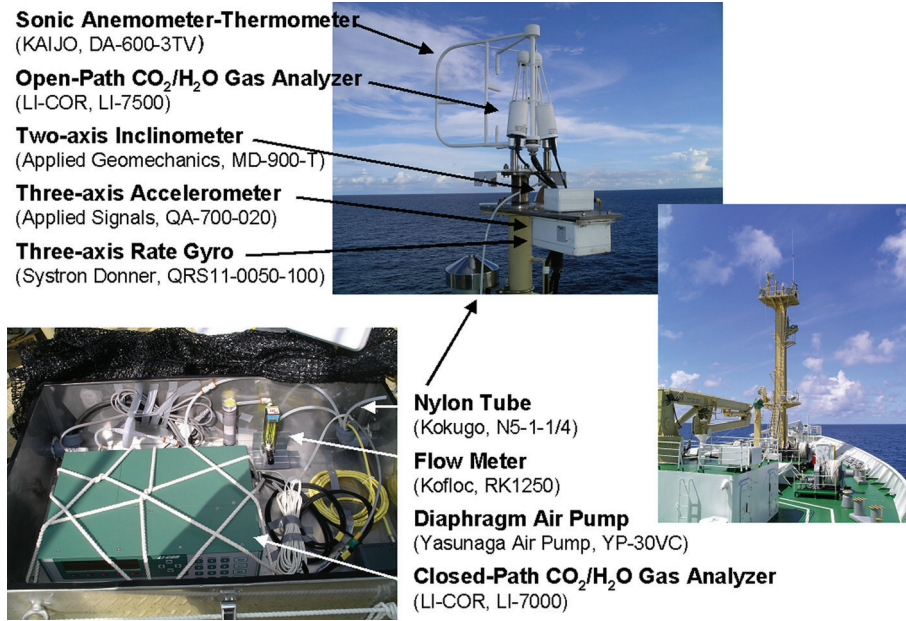
Fig. 1. Systems for turbulent flux observation and ship motion correlation on top of the foremast of the R/V MIRAI, JAMSTEC during the MR08-03 cruise.

tube and the flow rate of the air pump, was 0.3 s. On the other hand, the actual CPGA lag times determined by the cross-correlation of signals from both SAT and CPGA were 1.0–1.4 s; the CPGA signals were shifted accordingly. The reference cell in the CPGA was filled with a magnesium perchlorate desiccant and compressed pure air gas at a flow rate of $50\,mL\,min^{-1}$ as zero gas. Serrano-Ortiz et al. (2008) reported that the contamination of the optical window of the OPGA results in errors in the absolute measurement of the CO_2 density. Prytherch et al. (2010) suggested that this contamination results in errors not only in the absolute CO_2 density but also in its fluctuation. In this study, we cleaned the LI-7500 optical windows before the observations to avoid contamination by salt particles and raindrops and checked the Automatic Gain Control value ('clean window' baseline value) before and after all the special observations presented in the next section. The ship motion correction system consisted of a two-axis inclinometer (Applied Geomechanics, MD-900-T) for measuring the pitching and rolling angles, a three-axis accelerometer (Applied Signals, QA-700-020) for measuring three accelerations and a three-axis rate gyro (Systron Donner, QRS11-0050-100) for measuring three angular rates.

The analogue output signals from these instruments were sampled and digitised at a rate of 100 Hz using analogue-to-digital converters (National Instruments, DAQCard-AI-16XE-50) and recorded at an average rate of 10 Hz using a data acquisition system (National

Instruments, LabVIEW 8.5) on a laptop computer. All the data processing were carried out after the observations. The fluxes and spectra by the OPEC and CPEC were calculated at 30-min intervals. The wind velocities measured by the SAT were corrected for ship motion following Takahashi et al. (2005) and were rotated into a coordinate system aligned with the mean wind (McMillen, 1988). The crosswind correction for the sound virtual temperature measured by the SAT was included (Hignett, 1992). A linear de-trending of low frequency was applied to the fluctuation in each parameter before calculating each flux. At high frequencies, the losses in the CO_2 and H_2O fluxes by the OPEC caused by the sensor separation between the OPGA and SAT were corrected by the bandpass covariance method, assuming that the ratio of each high frequency of the cospectrum of the raw CO_2 flux to the sensible heat flux is similar (Watanabe et al., 2000). This method has been attempted by many researchers (e.g. Högström et al., 1989; Verma et al., 1992; Grelle and Lindroth, 1996), and it has been accepted as a good method for correcting both the high-frequency flux losses due to the sensor separation (Ono et al., 2007) and the sampling tubing attenuation (Yasuda and Watanabe, 2001). For that reason, the CO_2 and H_2O flux losses for the CPEC in this study were also corrected using the same method.

The general meteorological data (air temperature, humidity, short- and long-wave radiation, wind speed and direction and air pressure) were measured at a height of approximately 24 m above the sea surface

with the Shipboard Oceanographic and Atmospheric Radiation measurement (SOAR) and Surface Meteorological observation (SMET) systems. The properties of the bulk seawater temperature and salinity were measured at a depth of approximately 4.5 m below the sea surface.

The fugacities of CO$_2$ in the air and bulk seawater were calculated from the seawater temperature, salinity and mole fractions of CO$_2$ in dry marine air and in dry air equilibrated with seawater, which were measured using an automated system with a closed-path CO$_2$ gas analyser (Murata and Takizawa, 2003). This automated system was operated in one-and-a-half hour cycles. Standard gasses, marine air and equilibrated air with surface seawater within the equilibrator in one cycle were analysed subsequently. The concentrations of the standard gases were 299.90, 349.99, 399.94 and 449.99 ppmv. The marine air was sampled at approximately 0.5 L min^{-1} from an inlet approximately 30 m above the sea surface at the bow of the ship. Equilibrated air was sampled at 0.7–0.8 L min^{-1} from a showerhead-type equilibrator, and the seawater for equilibration was taken from a depth of approximately 4.5 m at 5–6 L min^{-1}. These air were dried with the cooling unit, membrane dryer (Permapure, MD-110-72P) and desiccant holder containing Mg(ClO$_4$)$_2$. The precision of sea–air CO$_2$ fugacity difference (ΔfCO$_2$) measurements in this study was within 1.9 µatm.

2.4. Observation sites

The observations were conducted aboard the R/V MIRAI of the Japan Agency for Marine-Earth Science and Technology (JAMSTEC) during the MR08-03 cruise in the equatorial Pacific Ocean. The cruise track was from Guam to Sekinehama, and it is shown in Fig. 2. This cruise took place from 3 July 2008 through 6 August 2008. During the MR08-03 cruise, special times for the turbulent flux observation were set at the four stations as shown in Table 1. The first to third runs were performed at station A (147°E, EQ), the fourth run at station B (156°E, 5°S), the fifth run at station C (156°E, EQ) and the sixth run at station D (156°E, 2°N). During these runs, the vessel was steered into the wind at a constant speed of maximum 8 knots to maintain the ship heading and to eliminate ship body effects.

During each flux run, the mean wind speed was low to moderate, ranging from 2.5 to 5.2 m s^{-1}. Sea surface temperature was almost constant and higher than air temperature, and the mean sea–air temperature difference ($\Delta T_{sea-air}$) was small at +0.2 to +1.0°C. Relative humidity was also relatively constant during each flux run and had a narrow range from 69.3 to 77.0%. Atmospheric fCO$_2$ was almost constant during each flux run, and the sea surface fCO$_2$ was oversaturated with respect to the atmosphere. The mean ΔfCO$_2$ was +12.7 to +41.4 µatm. After cleaning the LI-7500 optical windows, no precipitation events were recorded during all the flux runs.
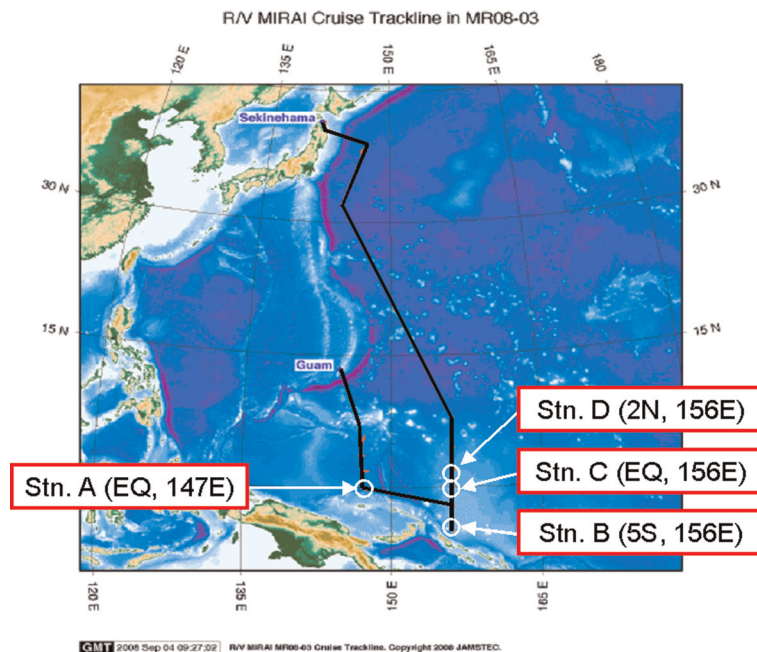

Fig. 2. Cruise track of the R/V MIRAI during MR08-03. This cruise took place from Guam (3 July 2008) to Sekinehama (6 August 2008), and it performed special observations for the flux measurements by the eddy covariance technique at the four (from A to D) stations.

Table 1. Station, position, day time, number (n) of fluxes measured by the eddy covariance technique, and mean values and SDs of wind speed, relative humidity, sea–air temperature difference ($\Delta T_{sea-air}$) and sea–air CO_2 fugacity difference (ΔfCO_2), during the turbulent flux observation runs performed at the four stations

Station	A			B	C	D
Position (latitude, longtitude)	EQ, 147°E			5°S, 156°E	EQ, 156°E	2°N, 156°E
Run	First	Second	Third	Fourth	Fifth	Sixth
Day time (MM/DD HH:MM)	07/09 12:00–18:00	07/10 07:00–19:00	07/11 08:30–19:30	07/16 07:30–17:30	07/20 07:30–17:30	07/22 07:30–18:00
n	9	15	17	15	18	16
Wind speed (m s^{-1})	2.9 ± 0.7	3.5 ± 0.6	4.2 ± 0.3	5.2 ± 0.5	5.4 ± 1.1	2.5 ± 0.7
Relative humidity (%)	75.7 ± 1.9	75.0 ± 1.7	71.3 ± 1.8	77.0 ± 1.1	69.3 ± 1.7	73.9 ± 1.8
$\Delta T_{sea-air}$ (°C)	+0.9 ± 0.2	+1.0 ± 0.4	+0.7 ± 0.1	+0.4 ± 0.1	+0.2 ± 0.2	+0.5 ± 0.1
ΔfCO_2 (µatm)	+20.5 ± 1.0	+23.9 ± 10	+24.7 ± 0.8	+12.7 ± 1.9	+34.3 ± 0.6	+41.5 ± 0.5

3. Results and discussion

3.1. Atmospheric turbulent fluctuations

Figure 3 shows a typical example of the atmospheric turbulent fluctuations of H_2O (ρ_{v_op}) and CO_2 (ρ_{c_op}) mass densities by the OPGA, and those of H_2O (ρ_{v_cl}) and CO_2 (ρ_{c_cl}) mass densities and H_2O (r_{v_cl}) and CO_2 (r_{c_cl}) mass mixing ratios by the CPGA. Note that all the fluctuations in Fig. 3 are plotted at 10 Hz raw data as the deviation from the mean value. In Fig. 3, ρ_{c_cl} and ρ_{v_cl} by the CPGA were converted from raw output signals (X_{c_cl} and X_{v_cl}, respectively) using the pressure and temperature in the sample cell. In addition, r_{v_cl} was converted using the method with which r_{c_cl} was calculated [eq. (6)].

ρ_{v_op} was positively correlated with the fluctuations of vertical wind velocity and sonic temperature. The maximum amplitude of ρ_{v_op} was approximately $1.6\,\mathrm{g\,m}^{-3}$. ρ_{v_cl} had almost the same amplitude as ρ_{v_op} while the fluctuation of ρ_{v_cl} in the high-frequency range attenuated in the sampling tube. ρ_{c_op} showed negative fluctuation with a maximum amplitude of approximately $-1.7\,\mathrm{mg\,m}^{-3}$ and was negatively correlated with the vertical wind velocity and sonic temperature fluctuations. The maximum amplitude of ρ_{c_cl} was smaller ($-1.2\,\mathrm{mg\,m}^{-3}$) than that of ρ_{c_op} because of the damped temperature fluctuation due to the WPL correction and attenuation of CO_2 density fluctuation itself. The CO_2 density fluctuations in the high-frequency range in the case of both OPGA and CPGA showed almost identical noise owing to the limiting sensitivity of these analysers to measure the small CO_2 density fluctuation over the ocean.

r_{v_cl} showed a positively skewed fluctuation as well as ρ_{v_cl}. r_{c_cl} showed a positively skewed fluctuation, but ρ_{c_cl} showed a negatively skewed fluctuation. Apparently, the CO_2 density fluctuation showed the contrary behaviour from the CO_2 mixing ratio under the significant influence

of air temperature and H_2O density fluctuations. Thus, in the present study, the total CO_2 flux by the OPEC changed sign due to the WPL correction, which is similar to the results given by previous studies (Ohtaki et al., 1989; Kondo and Tsukamoto, 2007).

Many observations over land have shown that there was a difference between the lag times for the CO_2 and H_2O fluctuations measured by the CPGA (Ibrom et al., 2007a). The lag time for the H_2O fluctuation was always longer than that for CO_2 fluctuation, and it can be determined empirically as the lag times with which the vertical wind velocity or air temperature fluctuations had to be shifted against both gas fluctuations. However, our observation did not show significant differences between both lag times (1.0–1.4 s) because a short sampling tube (3.2 m) and a high volume pump (12.0 L min^{-1}) were used for the air sampling. McGillis et al. (2004) suggested that the gyroscopic effect due to the ship motion caused false CO_2 signals with the CPGA technique and caused errors in the CO_2 flux. Miller et al. (2010) suggested that the CPGA is more sensitive to this effect than the OPGA. In this study, ship motion effects did not appear in both gas analysers because the motion cycles and magnitudes for our ship were comparatively slow and small during our cruise as shown in Figs. 3 and 4, respectively.

3.2. Spectral analysis

Figure 4 shows a typical example of the normalised power spectra of H_2O (left) and CO_2 (right) densities fluctuations measured by the OPGA and CPGA; that of the sonic temperature (T_s) fluctuation measured by the SAT are also shown. The ordinate on the logarithmic scale is the power spectral density $nS_{xx}(n)$ normalised by the variance σ^2 of each parameter x. The abscissa is the non-dimensional frequency $f = nz\,U^{-1}$ on a logarithmic scale. Here, n is the
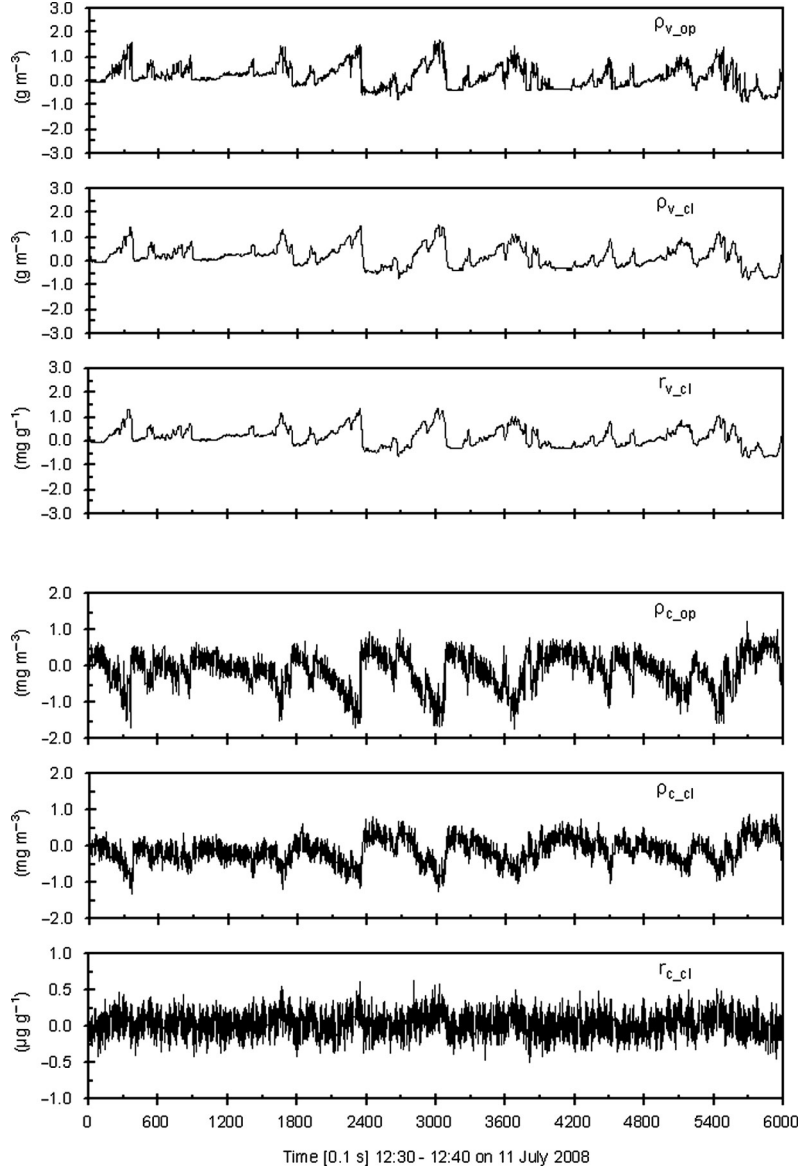
Fig. 3. A typical example of the atmospheric turbulent fluctuations for H$_2$O and CO$_2$ densities measured by the OPGA, and the H$_2$O and CO$_2$ densities and mixing ratios measured by the CPGA calculated with eqs. (6), (7) and (8). These fluctuations are plotted as a deviation from the mean value at 10 Hz.

frequency (Hz) and U is the mean wind speed (m s^{-1}) at the measurement height z (m).

These normalised power spectra had similar frequency structures over a wide frequency range below $f = 0.19$. The normalised power spectrum of ρ_{v_op} followed the $-2/3$ power law (the inertial subrange) in the wide frequency range ($0.05 < f < 1.54$), similar to T_s. The normalised power spectrum of ρ_{v_cl} also followed the $-2/3$ power law in the narrower frequency range ($0.05 < f < 0.19$) than that of ρ_{v_op}. Over the frequency range above $f = 0.19$, the normalised power spectrum of ρ_{v_cl} was considerably lower than that of ρ_{v_op} due to the sampling tube attenuation.

The normalised power spectrum of ρ_{c_op} as well as that of ρ_{v_op}, where the white noise appeared, followed the $-2/3$ power law in the frequency range ($0.05 < f < 1.54$). The normalised power spectrum of ρ_{c_cl} followed the $-2/3$ power law over the same frequency range ($0.05 < f < 0.19$) as that of ρ_{v_cl}. Moreover, the attenuation of ρ_{c_cl} in the sampling tube appeared in the frequency range of $0.19 < f < 0.97$, while the white noises of ρ_{c_cl} and ρ_{c_op} appeared over the frequency range above $f = 0.97$.

Figure 5 shows a typical example of the normalised cospectra of the above-mentioned parameters and the vertical wind velocity measured by the SAT as a function
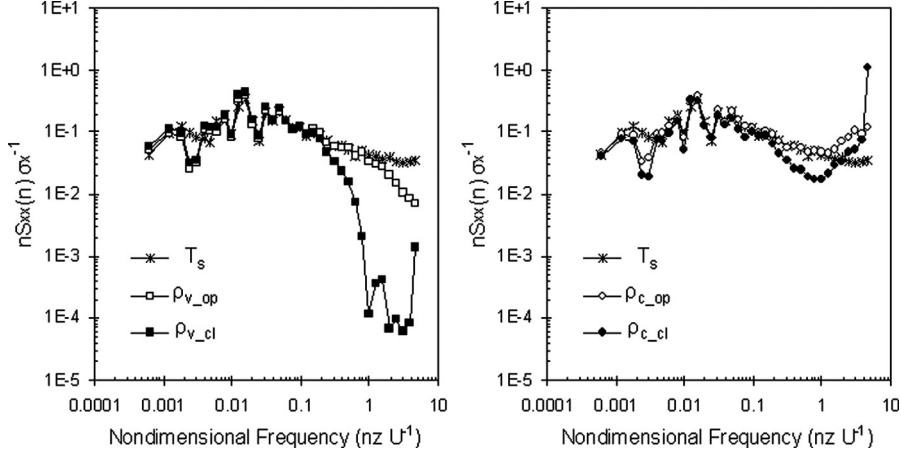
Fig. 4.   A typical example of the normalised power spectra of H_2O (left) and CO_2 (right) densities fluctuations measured by the open-path [open square (left) and open circle (right)] and closed-path [closed square (left) and closed circle (right)] CO_2/H_2O gas analysers; normalised power spectra of the sonic temperature fluctuations (cross) measured by the SAT.

of the non-dimensional frequency. The ordinate is the cospectrum $nC_{wx}(n)$, normalised by the flux $(\overline{w'x'})$ of each parameter. Each flux is equivalent to a frequency integral of the cospectrum $[C_{wx}(n)]$ of each parameter. The cospectra of the H_2O and CO_2 fluxes by the CPEC without the frequency correction are shown in Fig. 5. The shapes of the normalised cospectra of the H_2O and CO_2 fluxes were basically similar over a wide frequency range below $f = 0.1$ as well as that of the normalised cospectrum of the sensible heat flux. This indicates that the assumption of spectral similarity between the CO_2 (or H_2O) flux and sensible heat flux was satisfied, and further, that the bandpass covariance method for the flux correction can be useful. The most dominant frequency range in the cospectra of CO_2 fluxes by the OPEC and CPEC was centred at $f = 0.016$, as were the cospectra of H_2O fluxes. The cospectra of the CO_2 fluxes by both the OPEC and CPEC did not show the effect of white noise, which appeared only in the high-frequency

range (Fig. 4). This was because the instrumental white noise of the CO_2 density fluctuation did not correlate with the vertical wind velocity fluctuation. The ratio of the CO_2 (or H_2O) flux loss caused by the sampling tubing attenuation to the flux in the CPEC, corrected by the bandpass covariance method, was 5.0% for CO_2 (2.1–9.1%) and 4.2% for H_2O (3.0–5.8%) fluxes on an average when using the short sampling tube (3.2 m) and high volume pump (12.0 L min^{-1}).

3.3. CO_2 fluxes by the OPEC and CPEC techniques

Figure 6 shows the time-series data of the raw CO_2 flux (Raw), the WPL CO_2 correction terms due to air temperature fluctuations (*WPL for SHF*) and latent heat flux (*WPL for LHF*), and the total CO_2 flux by the OPEC [F_c(OPEC)], and the CO_2 flux by the CPEC [F_c(CPEC)] during the second run at station A on 10 July 2008.
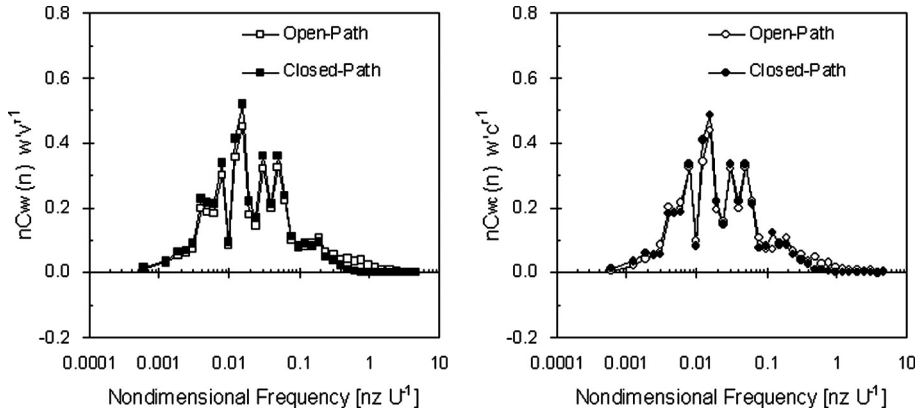

Fig. 5.   A typical example of the normalised cospectra of H_2O (left) and CO_2 (right) fluxes by the OPEC and CPEC as a function of the non-dimensional frequency. Each flux is equivalent to a frequency integral of the cospectrum of each parameter.
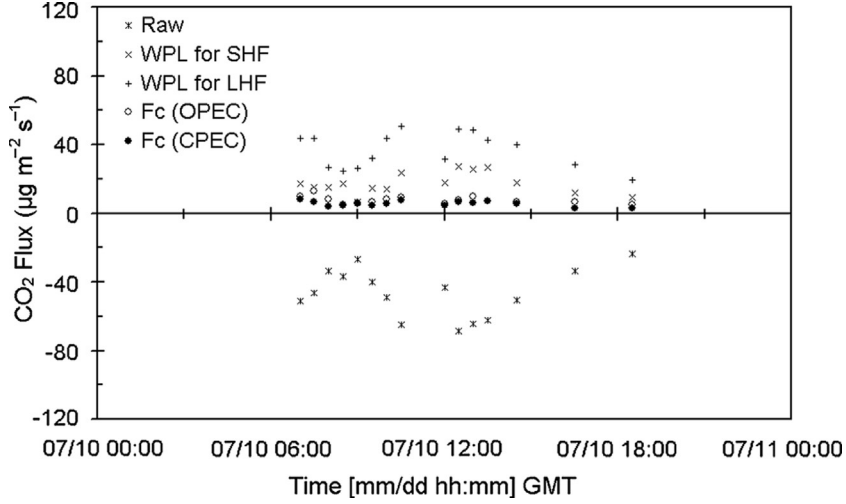
Fig. 6. Time-series data of raw CO$_2$ flux (*Raw*, asterisk), the WPL CO$_2$ correction terms for sensible (*WPL for SHF*, cross) and latent (*WPL for LHF*, plus) heat fluxes and total CO$_2$ flux by the OPEC [F_c(OPEC), open circle], and the CO$_2$ flux by the CPEC [F_c(CPEC), closed circle] at station A on 10 July 2008.

The raw CO$_2$ flux by the OPEC was an apparent sink and varied from -68.63 to $23.44 \mu g\,m^{-2}\,s^{-1}$. The WPL correction term for sensible heat flux was always positive and between $+6.63$ and $+27.24 \mu g\,m^{-2}\,s^{-1}$ (the sensible heat flux was between $+3.4$ and $+15.0\,W\,m^{-2}$). The WPL correction term for latent heat flux was between $+19.11$ and $+59.61 \mu g\,m^{-2}\,s^{-1}$ (the latent heat flux was between $+51.4$ and $+161.6\,W\,m^{-2}$). The total CO$_2$ flux by the OPEC became source ($+4.81$ to $+13.02 \mu g\,m^{-2}\,s^{-1}$) after the WPL correction was applied. The CO$_2$ flux by the CPEC was also source in the range of $+3.10$ to $+8.02 \mu g\,m^{-2}\,s^{-1}$ and somewhat smaller than the total CO$_2$ flux by the OPEC. Figure 7 shows the point by point comparison of total CO$_2$ flux by the OPEC and CO$_2$ flux by the CPEC measured during all special observation times. The total CO$_2$ flux by the OPEC was on average 20% larger than the CO$_2$ flux by the CPEC with the offset of $2.96 \mu g\,m^{-2}\,s^{-1}$; however, its coefficient of determination (R^2) was low (0.52).

We estimated the bulk CO$_2$ flux at each station using the mean wind speed and ΔfCO$_2$ when the flux observation runs were performed for approximately half a day. In this study, the data covered a narrow range of mean wind speed (2.9–$5.4\,m\,s^{-1}$) and mean ΔfCO$_2$ ($+12.7$ to $+41.4 \mu atm$), which drives the source CO$_2$ flux from the ocean to air at each station. Our results showed that both the CO$_2$ fluxes directly evaluated by the OPEC and CPEC had the same sign as the estimated bulk CO$_2$ flux, but were an order of magnitude larger than the bulk CO$_2$ fluxes ($+0.27$ to $+1.56 \mu g\,m^{-2}\,s^{-1}$), as shown in Table 2.

There are many possible reasons for the systematic errors in the CO$_2$ flux by the eddy covariance technique (e.g. tilt correction, block-averaging, de-trending, flow distortion, change in calibration coefficient and cross-sensitivity performance). The tilt correction, block-averaging and de-trending involved low-frequency contributions to the CO$_2$ flux, but the contributions were relatively small, as shown in Fig. 5. Secondly, the flow distortion is mainly sensitive to the momentum flux because it requires corrections to both the vertical and horizontal velocities, and results in even the momentum flux with an uncertainty of
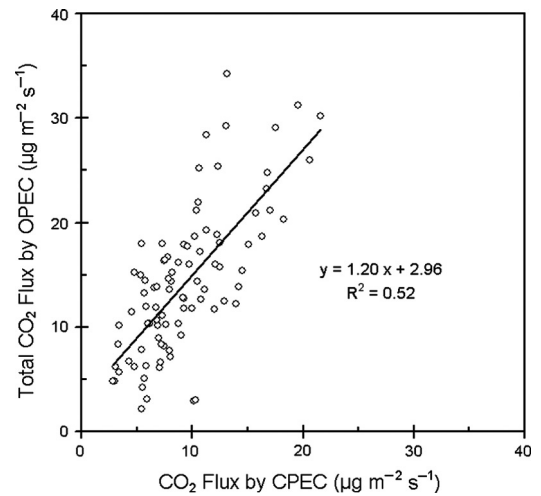

Fig. 7. Point by point comparison of total CO$_2$ flux by the OPEC and CO$_2$ flux by the CPEC measured during all special observation times.

Table 2.   Mean values of raw CO_2 flux by the OPEC, WPL CO_2 correction terms for sensible (*WPL for SHF*) and latent (*WPL for LHF*) heat fluxes by the OPEC, and total CO_2 flux by the OPEC, the CO_2 flux by the CPEC and bulk CO_2 flux estimated using the gas transfer velocity proposed by Wanninkhof (1992) during the turbulent flux observation runs performed at the four stations

Run	First	Second	Third	Fourth	Fifth	Sixth
Raw flux by OPEC ($\mu g\,m^{-2}\,s^{-1}$)	-43.85	-46.34	-56.53	-43.89	-60.50	-31.12
WPL for LHF by OPEC ($\mu g\,m^{-2}\,s^{-1}$)	$+33.28$	$+36.67$	$+48.40$	$+42.52$	$+55.31$	$+27.65$
WPL for SHF by OPEC ($\mu g\,m^{-2}\,s^{-1}$)	$+17.30$	$+17.34$	$+22.65$	$+19.24$	$+19.19$	$+11.35$
Total flux by OPEC ($\mu g\,m^{-2}\,s^{-1}$)	$+6.73$	$+7.66$	$+14.52$	$+17.87$	$+13.95$	$+7.74$
Flux by OPEC ($\mu g\,m^{-2}\,s^{-1}$)	$+6.71$	$+5.46$	$+8.87$	$+7.89$	$+9.78$	$+8.73$
Bulk flux ($\mu g\,m^{-2}\,s^{-1}$)	$+0.27$	$+0.46$	$+0.68$	$+0.54$	$+1.56$	$+0.40$

approximately 10–20% (Edson et al., 1998). In the case of the changes in the calibration coefficient and cross-sensitivity performance (Serrano-Ortiz et al., 2007; Prytherch et al., 2010), we made special efforts such as cleaning the OPGA optical windows to avoid contamination by salt particles and raindrops before the special times of turbulent flux observations analysed in this article. In the 1980s discussions, the traditional mismatch between the bulk CO_2 flux by the mass balance technique and the CO_2 flux by the eddy covariance technique was ascribed to the different time and space scales. On the other hand, we believed that this 1980s mismatch was the main cause of the uninvestigated sea salt contamination of the optical window of OPGA. Nevertheless, our results have shown that there is a mismatch between the bulk CO_2 flux and the CO_2 flux by the CPEC in addition to the total CO_2 flux by the OPEC, which were carefully take care to this contamination like our previous comparison study (Kondo and Tsukamoto, 2007). However, the mismatch in this study is absolutely smaller than the previous 1980s one.

McGillis et al. (2001) and Miller et al. (2010) suggested that the CO_2 flux over oceans be measured by the CPEC in order to eliminate a major source of uncertainty, i.e. the WPL correction. In this study, the WPL correction had significant effects and changed the sign of the CO_2 flux by the OPEC; this was the case in a previous study as well (Kondo and Tsukamoto, 2007). This correction caused a somewhat random error between the CO_2 fluxes by the OPEC with WPL correction and the CPEC without WPL correction; however, it did not cause a systematic error, as shown in Fig. 6. In addition, it has been proved that the theory of WPL correction is not contradictory from previous arguments (Massman and Tuovinen, 2006; Leuning, 2007).

The frequency correction has been identified to be crucial in the processing, especially for the evaluation of small CO_2 fluxes over the ocean by the CPEC. This correction for flux losses depends on the measurement height, wind speed and airflow rates (pump volume) and the dimensions (length and size) of the sampling tube used to sample the air for the

CPEC (Leuning and Moncrieff, 1990). Our results have shown that its relatively smaller contribution was 5.0% for CO_2 and 4.2% for H_2O over the ocean if our closed-path system comprised the minimum sampling tube length and the higher volume pump. Significant frequency response correction was required because the CO_2 flux loss contributions are likely to increase when using longer sampling tubes as the previous closed-path measurements over the ocean.

The air–sea bulk CO_2 flux can be estimated by the in situ measured parameters of the sea–air CO_2 fugacity difference, the air and sea surface water temperatures, salinity and wind speed as empirical function of the gas transfer velocity. In this study, each precision of these parameters did not fill the gap between the CO_2 flux by the eddy covariance technique and the bulk CO_2 flux. The primary cause of uncertainties when calculating the bulk CO_2 flux is the uncertain gas transfer velocity. The parameterisation of the CO_2 gas transfer velocity that is itself plotted against the wind speed alone is still problematic. The gas transfer velocity is influenced by a number of processes, but the wind speed has been shown to be the variable that explains the variations in the global gas flux from a practical standpoint. However, such parameterisation is too simplistic, and the scatter of each plot is extremely large over a wide wind speed range. Furthermore, the existing estimations of the gas transfer velocity under the low wind speed (especially, $<4\,m\,s^{-1}$) conditions, such as the conditions in this study, are insufficient. Recently, Sarma et al. (2010) proposed a novel mass balance technique using stable oxygen isotopes for the direct estimation of the gas transfer velocity and showed that the gas transfer velocity at low wind speeds was higher than the wind speed parameterised estimates based on previous tracers. From comparison of the CO_2 fluxes by the eddy covariance technique during this cruise, we believe the bulk CO_2 flux estimated using this parameterised gas transfer velocity is considerably smaller than that estimated in previous comparison studies. The CO_2 flux by the eddy covariance technique is within the scatter of bulk CO_2 flux involved in the gas transfer

velocity estimated by the mass balance technique, although significant differences between the results for both fluxes have been noted.

4. Conclusion

Direct measurements of trace gas fluxes by the eddy covariance technique over coastal seas and open oceans can potentially improve our understanding of the air–sea gas flux caused by various physical and chemical processes, and consequently, improve the precision of the estimated bulk trace gas flux. In this study, we have focused on directly comparing the CO$_2$ fluxes by OPEC and CPEC over the equatorial Pacific Ocean. Previous studies over oceans deduced a discrepancy between the CO$_2$ fluxes by both techniques via the bulk CO$_2$ flux estimated by the mass balance technique. Our primary results, obtained during the special time for the turbulent flux observations with the cleaning of OPGA optical window to avoid contamination by salt particles and raindrops, are summarised as follows.

The sign of the CO$_2$ flux by the OPEC changed from sink to source due to the significant WPL correction, as in the previous study. The apparent CO$_2$ density or net mixing ratio fluctuation can be measured by the CPGA with a short sampling tube and high volume air pump. The underestimation of the CO$_2$ flux in the high frequencies, which is caused by the attenuation of the CO$_2$ fluctuation in the sampling tube, is approximately 5.0% and can be fully corrected by the bandpass covariance method. Our results over the equatorial Pacific Ocean show a good agreement between the CO$_2$ fluxes by the OPEC and CPEC, and they are larger than the bulk CO$_2$ flux estimated using the gas transfer velocity, which was evaluated by mass balance technique.

5. Acknowledgements

References

Edson, J. B., Hinton, A. A., Prada, K. E., Hare, J. E. and Fairall, C. W. 1998. Direct covariance flux estimates from mobile platforms at sea. *J. Atmos. Ocean. Technol.* **15**, 547–562.

Grelle, A. and Lindroth, A. 1996. Eddy-correlation system for long-term monitoring of fluxes of heat, water vapor and CO$_2$. *Glob. Change Biol.* **2**, 297–307.

Hignett, P. 1992. Corrections to temperature measurements with a sonic anemometer. *Boundary-Layer Meteorol.* **61**, 175–187.

Högström, U., Bergström, H., Smedman, A.-S., Halldin, S. and Lindroth, A. 1989. Turbulent exchange above a pine forest, I: fluxes and gradients. *Boundary-Layer Meteorol.* **49**, 197–217.

Ibrom, A., Dellwik, E., Jensen, N. O., Flyvbjerg, H. and Pilegaard, K. 2007a. Strong low-pass filtering effects on water vapour flux measurements with closed-path eddy correlation systems. *Agric. For. Meteorol.* **147**, 140–156.

Ibrom, A., Dellwik, E., Larsen, S. E. and Pilegaard, K. 2007b. On the use of the Webb–Pearman–Leuning theory for closed-path eddy correlation measurements. *Tellus* **59B**, 937–946.

Jacobs, C. M. J., Kohsiek, W. and Oost, W. A. 1999. Air-sea fluxes and transfer velocity of CO$_2$ over the North Sea: results from ASGAMAGE. *Tellus* **51B**, 629–641.

Jones, E. P. and Smith, S. D. 1977. A first measurement of sea-air CO$_2$ flux by eddy correlation. *J. Geophys. Res.* **82**, 5990–5992.

Kondo, F. and Tsukamoto, O. 2007. Air-sea CO$_2$ flux by eddy covariance technique in the equatorial Indian Ocean. *J. Oceanogr.* **63**, 449–456.

Lee, X., Black, A. and Novak, M. D. 1994. Comparison of flux measurements with open- and closed-path gas analyzers above an agricultural field and a forest floor. *Boundary-Layer Meteorol.* **67**, 195–202.

Lenschow, D. H. and Raupach, M. R. 1991. The attenuation of fluctuations in scalar concentration through sampling tubes. *J. Geophys. Res.* **96D**, 15259–15268.

Leuning, R. 2007. The correct form of the Webb, Pearman and Leuning equation for eddy fluxes of trace gases in steady and non-steady state, horizontally homogeneous flows. *Boundary-Layer Meteorol.* **123**, 263–267.

Leuning, R. and King, K. M. 1992. Comparison of eddy-covariance measurements of CO$_2$ fluxes by open- and closed-path CO$_2$ analysers. *Boundary-Layer Meteorol.* **59**, 297–311.

Leuning, R. and Moncrieff, J. 1990. Eddy-covariance CO$_2$ flux measurements using open- and close-path CO$_2$ analysers: corrections for analyzer water vapour sensitivity and damping of fluctuations in air sampling tubes. *Boundary-Layer Meteorol.* **53**, 63–76.

Liss, P. S. and Merlivat, L. 1986. Air-sea gas exchange rates: introduction and synthesis. In: *The role of air-sea exchange in geochemical cycles* (eds. P. Buat-Manard and D. Reidel). Norwell, MA, pp. 113–127.

Massman, W. J. and Tuovinen, J.-P. 2006. An analysis and implications of alternative methods of deriving the density

(WPL) terms for eddy covariance flux measurements. *Boundary-Layer Meteorol.* **121**, 221–227.

McGillis, W. R., Edson, J. B., Hare, J. E. and Fairall, C. W. 2001. Direct covariance air-sea CO_2 fluxes. *J. Geophys. Res.* **106C**, 16729–16745.

McGillis, W. R., Edson, J. B., Zappa, C. J., Ware, J. D., McKenna, S. P. and co-authors. 2004. Air-sea CO_2 fluxes in the equatorial pacific. *J Geophys. Res.* **109**, C08S02. DOI: 10.1029/2003JC002256.

McMillen, R. T. 1988. An eddy correlation technique with extended applicability non-simple terrain. *Boundary-Layer Meteorol.* **43**, 231–245.

Miller, S. D., Marandino, C. and Saltzman, E. S. 2010. Ship-based measurement of air-sea CO_2 exchange by eddy covariance. *J Geophys. Res.* **115**, D02304. DOI: 10.1029/2009JD012193.

Murata, A. and Takizawa, T. 2003. Summertime CO_2 sinks in shelf and slope waters of the western Arctic Ocean. *Cont. Shelf Res.* **23**, 753–776.

Ohtaki, E., Tsukamoto, O., Iwatani, Y. and Mitsuta, Y. 1989. Measurements of the carbon dioxide flux over the ocean. *J. Meteorol. Soc. Japan* **67**, 541–554.

Ono, K., Hirata, R., Mano, M., Miyata, A., Saigusa, N. and co-authors. 2007. Systematic differences in CO_2 fluxes measured by open- and closed-path eddy covariance systems: influence of air density fluctuations resulting from temperature and water vapor transfer. *J. Agric. Meteorol.* **63**, 139–155.

Prytherch, J., Yelland, M. J., Pascal, R. W., Moat, B. I., Skjelvan, I. and co-authors. 2010. Direct measurements of the CO_2 flux over the ocean: development of a novel method. *Geophys. Res. Lett.* **37**, L03607. DOI: 10.1029/2009GL041482.

Sahlée, E. and Drennan, W. M. 2009. Measurements of damping of temperature fluctuations in a tube. *Boundary-Layer Meteorol.* **132**, 339–348.

Sarma, V. V. S. S., Abe, O., Honda, M. and Saino, T. 2010. Estimating of gas transfer velocity using triple isotopes of dissolved oxygen. *J. Oceanogr.* **66**, 505–512.

Serrano-Ortiz, P., Kowalski, A. S., Domingo, F., Ruiz, B. and Alados-Arboledas, L. 2008. Consequences of uncertainties in CO_2 density for estimating net ecosystem CO_2 exchange by open-path eddy covariance. *Boundary-Layer Meteorol.* **126**, 209–218.

Serrano-Oriz, P., Kowalski, A. S., Domingo, F., Ruiz, B. and Alados-Arboledas, L. 2007. Consequences of uncertainties in CO_2 density for estimating net ecosystem CO_2 exchange by open-path eddy covariance. *Boundary-Layer Meteorol.* **126**, 209–218.

Smith, S. D. and Jones, E. P. 1985. Evidence for wind-pumping of air-sea gas exchange based on direct measurements of CO_2 fluxes. *J. Geophys. Res.* **90C**, 869–875.

Suyker, A. E. and Verma, S. B. 1993. Eddy correlation measurements of CO_2 flux using a closed-path sensor: theory and field test against an open-path sensor. *Boundary-Layer Meteorol.* **64**, 391–407.

Takahashi, S., Kondo, F., Tsukamoto, O., Ito, Y., Hirayama, S. and co-authors. 2005. On-board automated eddy flux measurement system over open ocean. *SOLA* **1**, 37–40.

Verma, S. B., Ullman, F. G., Billesbach, D., Clement, R. J.,Kim, J. and co-authors. 1992. Eddy correlation measurements of methane flux in a northern peatland ecosystem. *Boundary-Layer Meteorol.* **58**, 289–304.

Wanninkhof, R. 1992. Relationship between wind speed and gas exchange over the ocean. *J. Geophys. Res.* **97C**, 7373–7382.

Watanabe, T., Yamanoi, K. and Yasuda, Y. 2000. Testing of the bandpass eddy covariance method for a long-term measurement of water vapour flux over a forest. *Boundary-Layer Meteorol.* **96**, 473–491.

Webb, E. K., Pearman, G. I. and Leuning, R. 1980. Correlation of flux measurement for density effects due to heat and water vapour transfer. *Q. J. R. Meteorol. Soc.* **106**, 85–100.

Weiss, R. F. 1974. Carbon dioxide in water and seawater: the solubility of a non-ideal gas. *Mar. Chem.* **2**, 203–215, DOI:10.1016/0304-4203(74) 90015-2.

Yasuda, Y. and Watanabe, T. 2001. Comparative measurements of CO_2 flux over a forest using closed-path and open-path CO_2 analysers. *Boundary-Layer Meteorol.* **100**, 191–208.